Landslide susceptibity mapping using Analytical Hierarchy Process and Fuzzy-Analytical Hierarchy Process approches: A case study in Binh Dinh province, Viet Nam

Đinh Thị Linh[1], Phùng Đại Khánh[2,3,*], Lê Trung Chơn[1], Huỳnh Quyền[1]

[1]*The Ho Chi Minh city University of Natural Resources and Environment, Vietnam*

[2]*Sejong University, Seoul, South of Korea*

[3]*South Vietnam Marine and Geological Mapping Division, Ho Chi Minh city, Vietnam*

[*] *Corresponding Author Email: phungdaikhanh@gmail.com*

https://doi.org/10.5281/zenodo.18476916

Abstract:

Binh Dinh Province, Vietnam, has recently experienced frequent landslide events, highlighting the urgent need for effective hazard assessment. This study aims to evaluate landslide susceptibility using the Analytical Hierarchy Process (AHP) and Fuzzy Analytical Hierarchy Process (Fuzzy-AHP) models. Ten conditioning factors were considered in both models: elevation, slope, aspect, Topographic Wetness Index (TWI), Standardized Precipitation Index (SPI), Normalized Difference Vegetation Index (NDVI), Normalized Difference Water Index (NDWI), distance to roads, distance to rivers, and geological characteristics. The resulting susceptibility maps were classified into five categories: very low, low, moderate, high, and very high. Model validation was conducted using the Receiver Operating Characteristic (ROC) curve, with Area Under the Curve (AUC) values exceeding 0.80, Root Mean Square Error (RMSE) values around 0.2, and accuracy scores above 0.8 for both models—indicating excellent predictive performance. Notably, the Fuzzy-AHP model slightly outperformed the AHP model. The analysis revealed that approximately 15% of the area falls within high and very high susceptibility zones, 30% within the moderate zone, and the remaining areas within low or very low susceptibility zones. These findings confirm the effectiveness and reliability of both the AHP and Fuzzy-AHP approaches for landslide susceptibility assessment. The resulting maps provide valuable guidance for local authorities and stakeholders in implementing disaster risk reduction strategies, early warning systems, and sustainable land-use planning.

Key words: *Landslides susceptibility mapping (LSM), Analytical Hierarchy Process (AHP), Fuzzy Analytical Hierarchy Process (Fuzzy-AHP), Multi-criteria decision analysis (MCDA).*

Submission received: 10/10/2025 Revised: 30/10/2025 Accepted: 14/11/2025 Published: 31/12/2025

1. Introduction

Landslides are significant natural disasters that occur worldwide, causing substantial impacts on society and the economy. Global landslide fatality data recorded 55,997 deaths from 2004 to 2016, with 9,223 landslides reported between 2000 and 2020. According to Froude and Petley [1], 75% of these landslides occurred in Asia, with India experiencing the highest number of incidents.

In recent years, various approaches for landslide susceptibility map have been studied, such as fuzzy logic [2], frequency ratio [3], analytical network process [4], FROC [5]. Researchers have also applied machine learning and deep learning models for landslide susceptibility modeling, including support vector machine (SVM), decision tree [6], K-nearest neighbor [7], random forest (RF) [8], adaptive neuro-fuzzy inference system (ANFIS) [9], convolutional neural network [10], logistic regression,… Furthermore, some ensemble machine learning methods,

such as genetic algorithm, boosted regression tree, logistic model tree, and Particle Swarm Optimization [11], have also been explored for landslide susceptibility mapping. The effectiveness and efficiency of machine learning approaches are determined by the type and the quality of data, as well as the performance of the learning algorithm [11].

In addition to machine learning algorithms, traditional methods based on decision-makers also play a crucial role. These approaches break down complex problems into specific sub-issues through pairwise comparisons, a process known as multi-criteria decision analysis (MCDA). The Analytic Hierarchy Process (AHP) is a widely used MCDA method for decision-making across various fields, while Fuzzy-AHP is a refined version of AHP. A key advantage of AHP and Fuzzy-AHP is their suitability in situations where large datasets of landslides are not available for training and validation [11]. Furthermore, these methods can deliver more reliable results in data-scarce conditions compared to machine learning techniques. Therefore, applying AHP and Fuzzy-AHP to landslide susceptibility mapping offers significant benefits.

The purpose of this study is to develop landslide susceptibility maps for Binh Dinh province, Viet Nam, using the AHP and Fuzzy-AHP methods. Additionally, the study compares the performance of these two methods to assess their applicability to the study area.

2. Study area and methods

2.1. Study area

The study area consists of three districts—Hoai An, Hoai Nhon, and An Lao—located in Binh Dinh Province, Vietnam (*Figure 2*). It spans an area of approximately 1,877.6 km², situated between 108°40' to 109°10' East longitude and 14°10' to 14°40' North latitude. The region experiences a tropical monsoon climate, with a rainy season from September to December and a dry season from January to August. The average annual rainfall is about 2,200 mm, and the mean annual temperature ranges from 20.1°C to 26.1°C, with recorded extremes of 16.5°C and 31.7°C.

In recent years, the area has witnessed an increasing frequency of landslide events. Notably, on November 23, 2024, a major landslide occurred at kilometer 13 of the inter-communal road linking An Lao Town to An Vinh Commune in An Lao District. Approximately 1,000 m³ of soil and rock from the uphill talus slope collapsed, completely obstructing the road. As this is the sole access route to the center of An Vinh Commune, all vehicular movement was disrupted.

Throughout An Lao District, nine transportation routes were impacted by landslides across eleven locations, displacing over 2,440 m³ of earth and rock. Additionally, approximately 122 m³ of concrete pavement was damaged or dislodged. The district's irrigation infrastructure also sustained significant damage, with around 4,200 meters of canals buried by debris and 33 m³ of concrete canal segments destroyed.

In Hoai An District, a 2,100-meter stretch of the An Lao River bank—from My Duc Hamlet to Long Quang Hamlet in An My Commune—experienced severe erosion, with collapse heights ranging from 8 to 9 meters. This erosion poses a serious threat to the safety and property of residents living along the river.

In Hoai Nhon Town, structural damage was observed along the Lai Giang River embankment near the Dinh Binh Pump Station. The embankment exhibited signs of cracking and subsidence, causing the pump station to tilt toward the river. This damage has jeopardized the stability of the water conveyance system and may affect its operational functionality.

Figure 1: *The landslide in An Lao district in November 23, 2024*

2.2. Data sources

Data sources used in this study include:

- SRTM DEM with a spatial resolution of 30m is downloaded from the USGS website (https://earthexplorer.usgs.gov/).
- Landsat 8 image with a spatial resolution of 30m is downloaded from the USGS website (https://earthexplorer.usgs.gov/).
- Geological map is collected from World Geologic Maps.
- Landslide locations are collected from Google Earth.
- Road and River systems are collected from Google Earth Pro.

2.3. Influencing factors

Numerous conditioning factors for landslides have been proposed by researchers, and selecting the appropriate factors is crucial for creating a reliable landslide susceptibility map that aligns with the data conditions of the study area. In this study, ten conditioning factors were considered: Elevation (DEM), slope, aspect, Topographic Wetness Index (TWI) and Standardized Precipitation Index (SPI), Normalized Difference Vegetation Index (NDVI) and Normalized

Difference Water Index (NDWI), distance to road, distance to river and Geology. The flowchart and data processing steps for this study are shown in Figure 3.

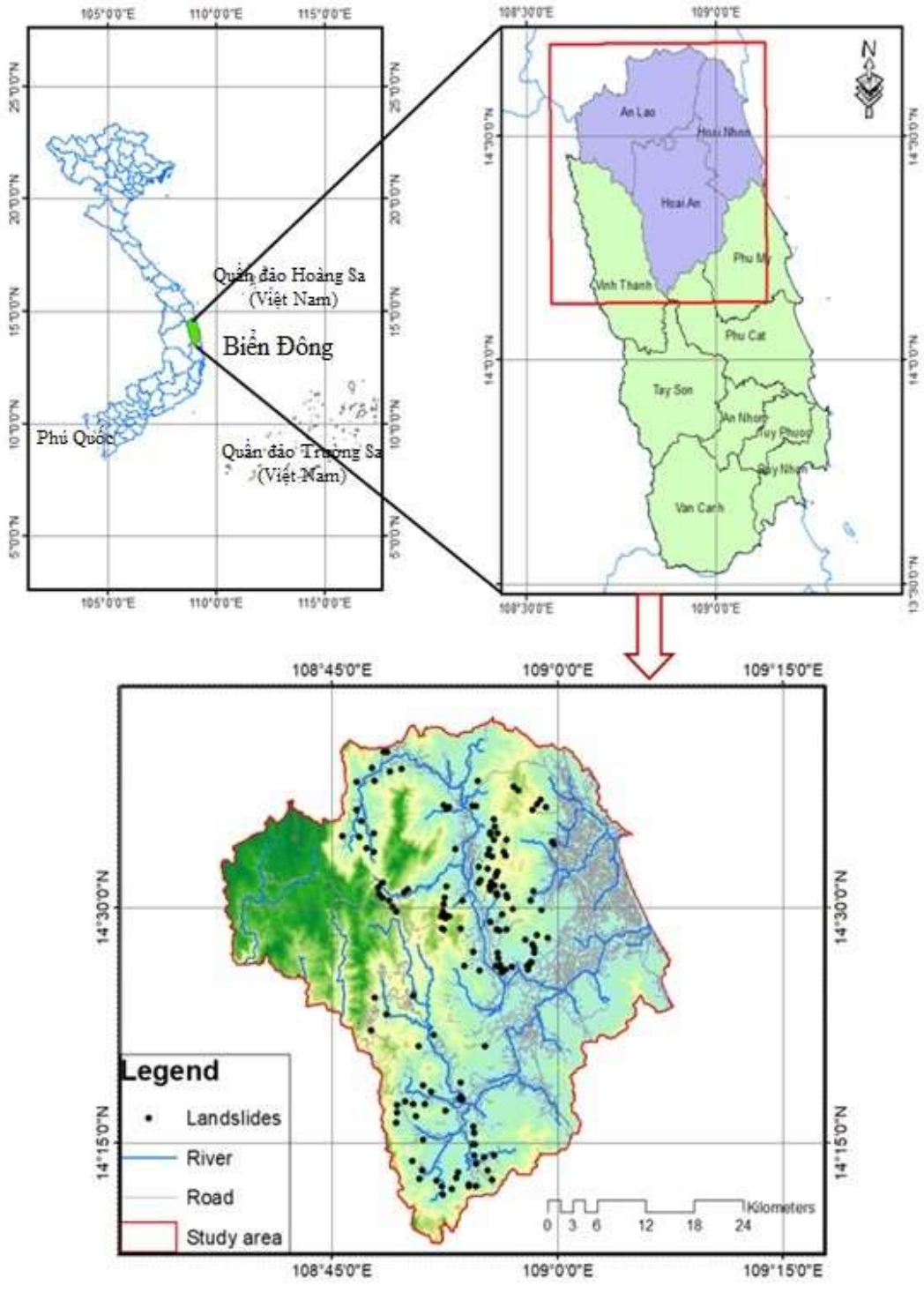

Figure 2: *Location of study area*

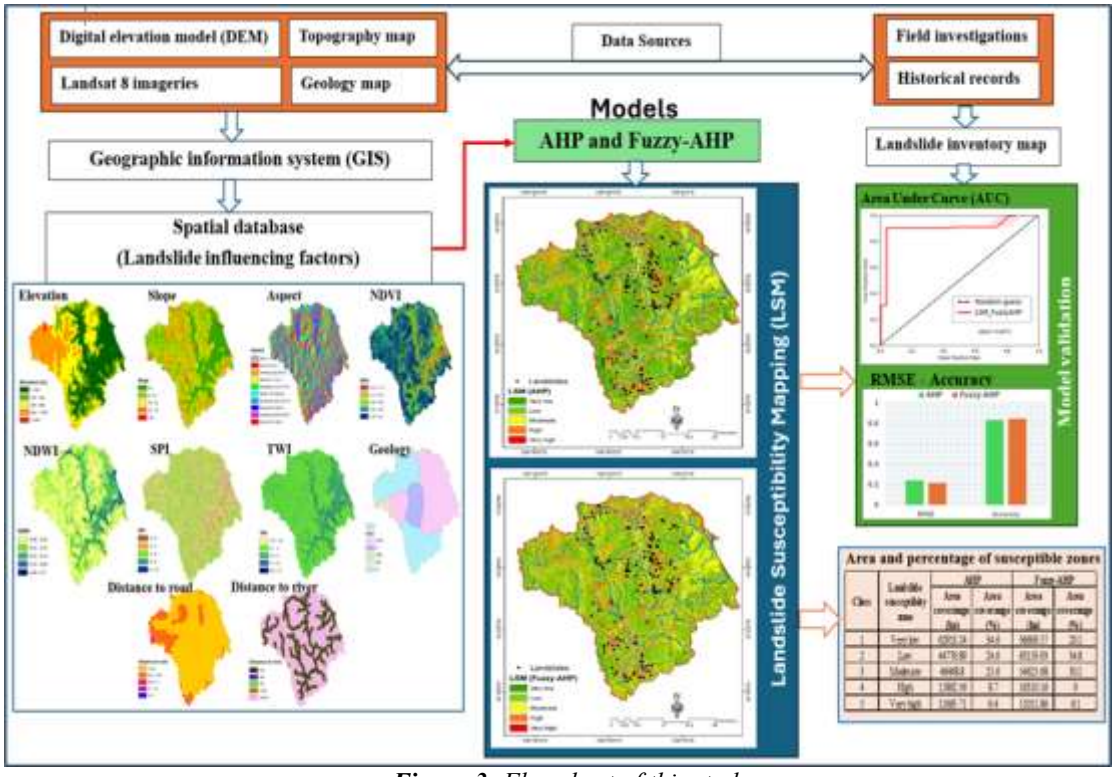

Figure 3: *Flowchart of this study*

2.4. Analytical Hierarchy Process (AHP)

The AHP is a type of Multi-Criteria Decision-Making (MCDM) method developed by Thomas [12]. This approach breaks down complex problems into a hierarchical structure to identify the best solution for a given goal. The key steps in this method involve creating a pairwise comparison matrix and calculating the weighting coefficients (Table 1). Nevertheless, pairwise comparisons are inherently subjective, and the quality of the results heavily relies on expert judgment [13]. To ensure consistency in expert decisions, a consistency ratio (CR) is used as a control measure (Table 2).

$$\mathrm{CR} = \frac{CI}{RI} \tag{1}$$

where RI is random index (=1.49) [12], CI is the consistency index which is described through λ_{max} and n (where λ_{max} is the largest eigenvalue of the matrix, n is the order of the matrix), If CR <0.1 is admissible, else the analysis is repeated.

$$CI = \frac{\lambda_{max} - n}{n-1} \tag{2}$$

According to the Equation, we calculate the λ_{max} value of 10.54, CI value of 0.06 and CR of 0.04. As a result, the CR value is accepted. Thus, the AHP weights are demonstrated as below:

LSM (AHP) = (0.29 × Elevation) + (0.21 × Slope) + (0.15 × Aspect) + (0.11 × NDVI) + (0.08 × NDWI) + (0.06 × TWI) + (0.04 × SPI) + (0.03 × Geology) + (0.02 × Distance to road) + (0.02 × Distance to river).

2.5. Fuzzy-Analytical Hierarchy Process (Fuzzy-AHP)

The Fuzzy-AHP approach combines Fuzzy Logic with the AHP method to weigh factors more effectively. It addresses the limitations of AHP by allowing decision-makers to express their preferences within a range, providing greater flexibility and reducing subjectivity [12]. The Fuzzy-AHP process can be summarized as follows: first, a pairwise comparison matrix is created (Table 3), followed by the computation of the geometric mean (Table 4) and the determination of fuzzy weights (Table 5). The final step involves calculating the averaged and normalized weights (Table 6). Further details of this method are presented by Bhagya [11].

Based on the obtained results, the Fuzzy-AHP weights are demonstrated as below:

LSM (Fuzzy-AHP) = (0.26 × Elevation) + (0.2 × Slope) + (0.156 × Aspect) + (0.116 × NDVI) + (0.085 × NDWI) + (0.062 × TWI) + (0.045 × SPI) + (0.033 × Geology) + (0.025 × Distance to road) + (0.019 × Distance to river).

2.6. Validation of the landslide susceptibility maps

2.6.1. ROC technique

In this study, a Receiver Operating Characteristic (ROC) technique is used to validate the landslide susceptibility maps. The ROC technique is a metric for evaluating classification performance[14]. The model's performance is considered outstanding if the Area Under the Curve (AUC) value ranges from 0.9 to 1.0, excellent between 0.8 and 0.9, and acceptable between 0.7 and 0.8 [15]. An AUC value below 0.7 indicates poor performance. The ROC and AUC values are computed using the Spatial Data Modeller (SDM) toolbox in ArcGIS.

$$\text{True Positive Rate (TPR)} = \frac{TP}{TP + FN} \tag{3}$$

$$\text{False Positive Rate (FPR)} = \frac{FP}{FP + TN} \tag{4}$$

$$\text{AUC} = \frac{1 + TPR - FPR}{2} \tag{5}$$

where TP is true positive, TN is true negative, FP is false positive and FN is false negative.

2.6.2. Accuracy

Moreover, accuracy was employed as a key performance metric in this study. It measures the proportion of correctly classified instances—both positive and negative—relative to the total number of instances. The accuracy was calculated using the following formula:

$$Accuracy = \frac{TP + TN}{TP + TN + FP + FN} \quad (6)$$

2.6.3. Root Mean Square Error (RMSE)

The Root Mean Square Error (RMSE) is defined as the square root of the mean of the squared differences between predicted and actual values, providing a comprehensive measure of model prediction accuracy [16]. In this study, RMSE was calculated as below:

$$RMSE = \sqrt{\frac{1}{n}\sum_{i=1}^{n}(X_i - \tilde{X}_i)^2} \quad (7)$$

Where X_i represents the predicted value, $\tilde{X}_i$ denotes the observed value, and n is the total number of observations or data points.

3. Results and discussion

3.1. Influencing factors

Elevation, derived from SRTM DEM, is a crucial factor in determining landslide susceptibility maps. It helps identify areas more prone to landslides, as higher elevations are generally more susceptible due to various contributing factors [17]. High spatial resolution elevation data is essential for producing reliable landslide susceptibility maps. In this study, elevation has been classified into five groups: very low (<100 m), low (100–300 m), moderate (300–600 m), high (600–1000 m), and very high (>1000 m) (Figure 4a).

Slope is a critical factor in developing landslide susceptibility maps, as steeper slopes are generally associated with a higher risk of landslides. It represents the steepness of the terrain surface and is typically derived from digital elevation models [17]. The slope has also been classified into 5 groups, including: <8º; 8-16º; 16-24º; 24-30º; and >30º (Figure 4b).

The Magazine of Geodesy - Cartography has been in operation since 1970.

Magazine of Geodesy – Cartography
Vol 11, N° Special (12/2025), ISSN: 2615-9481
Tạp chí Trắc địa - Bản đồ
Tập 11, Số Đặc biệt (12/2025), ISSN: 2615-9481

***Table 1**: Pairwise comparison matrix.*

	Elevation	Slope	Aspect	NDVI	NDWI	TWI	SPI	Geology	Distance to road	Distance to river
Elevation	1	2	3	4	5	6	7	8	9	10
Slope	1/2	1	2	3	4	5	6	7	8	9
Aspect	1/3	1/2	1	2	3	4	5	6	7	8
NDVI	1/4	1/3	1/2	1	2	3	4	5	6	7
NDWI	1/5	1/4	1/3	1/2	1	2	3	4	5	6
TWI	1/5	1/5	1/4	1/3	1/2	1	2	3	4	5
SPI	1/7	1/5	1/5	1/4	1/3	1/2	1	2	3	4
Geology	1/8	1/7	1/5	1/5	1/4	1/3	1/2	1	2	3
Distance to road	1/9	1/8	1/7	1/5	1/5	1/4	1/3	1/2	1	2
Distance to river	1/10	1/9	1/8	1/7	1/5	1/5	1/4	1/3	1/2	1
Total	**2.93**	**4.83**	**7.72**	**11.59**	**16.45**	**22.28**	**29.08**	**36.83**	**45.50**	**55.00**

***Table 2**: Normalized matrix*

	Elevation	Slope	Aspect	NDVI	NDWI	TWI	SPI	Geology	Distance to road	Distance to river	Criteria Weights
Elevation	0.34	0.41	0.39	0.35	0.30	0.27	0.24	0.22	0.20	0.18	**0.29**
Slope	0.17	0.21	0.26	0.26	0.24	0.22	0.21	0.19	0.18	0.16	**0.21**
Aspect	0.11	0.10	0.13	0.17	0.18	0.18	0.17	0.16	0.15	0.15	**0.15**
NDVI	0.09	0.07	0.06	0.09	0.12	0.13	0.14	0.14	0.13	0.13	**0.11**
NDWI	0.07	0.05	0.04	0.04	0.06	0.09	0.10	0.11	0.11	0.11	0.08
TWI	0.06	0.04	0.03	0.03	0.03	0.04	0.07	0.08	0.09	0.09	0.06
SPI	0.05	0.03	0.03	0.02	0.02	0.02	0.03	0.05	0.07	0.07	0.04
Geology	0.04	0.03	0.02	0.02	0.02	0.01	0.02	0.03	0.04	0.05	0.03
Distance to road	0.04	0.03	0.02	0.01	0.01	0.01	0.01	0.01	0.02	0.04	0.02
Distance to river	0.03	0.02	0.02	0.01	0.01	0.01	0.01	0.01	0.01	0.02	0.02
Total	1.00	1.00	1.00	1.00	1.00	1.00	1.00	1.00	1.00	1.00	**1.00**

Table 3. *Pair-wise comparison matrix*

	Elevation	Slope	Aspect	NDVI	NDWI	TWI	SPI	Geology	Distance to road	Distance to river
Elevation	(1,1,1)	(1,2,3)	(1,2,3)	(2,3,4)	(3,4,5)	(4,5,6)	(5,6,7)	(6,7,8)	(7,8,9)	(8,9,10)
Slope	(1/3,1/2,1)	(1,1,1)	(1,2,3)	(1,2,3)	(2,3,4)	(3,4,5)	(4,5,6)	(5,6,7)	(6,7,8)	(7,8,9)
Aspect	(1/3,1/2,1)	(1/3,1/2,1)	(1,1,1)	(1,2,3)	(1,2,3)	(2,3,4)	(3,4,5)	(4,5,6)	(5,6,7)	(6,7,8)
NDVI	(1/4,1/3,1/2)	(1/3,1/2,1)	(1/3,1/2,1)	(1,1,1)	(1,2,3)	(1,2,3)	(2,3,4)	(3,4,5)	(4,5,6)	(5,6,7)
NDWI	(1/5,1/4,1/3)	(1/4,1/3,1/2)	(1/3,1/2,1)	(1/3,1/2,1)	(1,1,1)	(1,2,3)	(1,2,3)	(2,3,4)	(3,4,5)	(4,5,6)
TWI	(1/6,1/5,1/4)	(1/5,1/4,1/3)	(1/4,1/3,1/2)	(1/3,1/2,1)	(1/3,1/2,1)	(1,1,1)	(1,2,3)	(1,2,3)	(2,3,4)	(3,4,5)
SPI	(1/7,1/6,1/5)	(1/6,1/5,1/4)	(1/5,1/4,1/3)	(1/4,1/3,1/2)	(1/3,1/2,1)	(1/3,1/2,1)	(1,1,1)	(1,2,3)	(1,2,3)	(2,3,4)
Geology	(1/8,1/7,1/6)	(1/7,1/6,1/5)	(1/6,1/5,1/4)	(1/5,1/4,1/3)	(1/4,1/3,1/2)	(1/3,1/2,1)	(1/3,1/2,1)	(1,1,1)	(1,2,3)	(1,2,3)
Distance to road	(1/9,1/8,1/7)	(1/8,1/7,1/6)	(1/7,1/6,1/5)	(1/6,1/5,1/4)	(1/5,1/4,1/3)	(1/4,1/3,1/2)	(1/3,1/2,1)	(1/3,1/2,1)	(1,1,1)	(1,2,3)
Distance to river	(1/10,1/9,1/8)	(1/9,1/8,1/7)	(1/8,1/7,1/6)	(1/7,1/6,1/5)	(1/6,1/5,1/4)	(1/5,1/4,1/3)	(1/4,1/3,1/2)	(1/3,1/2,1)	(1/3,1/2,1)	(1,1,1)

Table 4. *Geometric mean value of fuzzy comparison*

	Fuzzy Geometric Mean Value		
Elevation	2.89	3.86	4.72
Slope	2.10	2.89	3.75
Aspect	1.55	2.19	3.01
NDVI	1.13	1.61	2.28
NDWI	0.82	1.17	1.68
TWI	0.59	0.85	1.22
SPI	0.44	0.62	0.89
Geology	0.33	0.46	0.65
Distance to road	0.27	0.35	0.48
Distance to river	0.21	0.26	0.35

Table 5. *Relative fuzzy weights*

	Fuzzy Weight		
Elevation	0.15	0.27	0.46
Slope	0.11	0.20	0.36
Aspect	0.08	0.15	0.29
NDVI	0.06	0.11	0.22
NDWI	0.04	0.08	0.16
TWI	0.03	0.06	0.12
SPI	0.02	0.04	0.09
Geology	0.02	0.03	0.06
Distance to road	0.01	0.02	0.05
Distance to river	0.01	0.02	0.03

Table 6. *Averaged and normalized weights*

	Weight	Normalized Weight
Elevation	0.293	0.260
Slope	0.225	0.200
Aspect	0.175	0.156
NDVI	0.131	0.116
NDWI	0.096	0.085
TWI	0.070	0.062
SPI	0.051	0.045
Geology	0.037	0.033
Distance to road	0.028	0.025
Distance to river	0.021	0.019

Aspect represents the direction a slope faces, measured in degrees from 0° to 360°, and is typically derived from digital elevation models (DEMs) [17]. In landslide susceptibility mapping, aspect helps identify areas more prone to landslides by analyzing slope orientation. In this study, aspect is calculated in ArcGIS using the "3D Analyst" tools and classified into ten groups: Flat, North, Northeast, East, Southeast, South, Southwest, West, Northwest and North (Figure 4c).

The NDVI and NDWI are extracted from Landsat 8 with a spatial resolution of 30 x 30m. The NDVI is calculated utilizing red (R) and near-infrared (NIR) bands, while NDWI index is derived from the NIR and green (G) bands (Figure 4d and Figure 4e).

$$\text{NDVI} = \frac{NIR - R}{NIR + R} \tag{8}$$

$$\text{NDWI} = \frac{G - NIR}{G + NIR} \tag{9}$$

The SPI represents the erosive power of a river or stream, calculated using factors such as channel width, slope, and drainage area. SPI indicates the erosional force of surface water flow, making it a crucial hydraulic factor in landslide susceptibility mapping [17]. Higher SPI values suggest greater susceptibility to landslides due to increased erosion and terrain instability. The equation for computing the SPI index is presented as follows:

$$\text{SPI} = A * \tan\beta \tag{10}$$

where A is the area of the specific catchment, and β is the slope angle.

The SPI has also been classified in to 5 groups, including: -5 – 2; 2-4; 4-6; 6-8 and 8-10 (Figure 4f).

The TWI is a crucial hydrological factor in landslide studies, representing areas prone to saturation due to surface runoff influenced by topographic parameters [17]. The TWI is calculated using the following equation:

$$\text{TWI} = \ln\left(\frac{a}{\tan\beta}\right) \tag{11}$$

where a is the upslope contributing area per unit contour length, and β is the local slope angle. The calculated TWI values range from -15 to 12 (Figure 4g).

Geology provides essential information about rock types, soil types, and the geological characteristics of the study area. Geological data is typically obtained

from categorized geological maps, reflecting the terrain's structural features (Figure 4h).

Distance from rivers is another critical factor considered in this study. As the distance to a river decreases, groundwater influence and erosion caused by the river's force increase, heightening the probability of landslide occurrence [18]. In this study, the distance from river has been classified into 5 groups, including: <250m; 500-750m; 750-1000m; 1000-10000m (Figure 4i).

Anthropogenic factors refer to human activities such as vegetation removal, mining, and infrastructure development, which can contribute to landslides, especially due to the impact of road networks [19]. In this study, the distance from roads is analyzed and classified in ArcGIS, helping to assess the influence of human-made structures on landslide susceptibility. (Figure 4k).

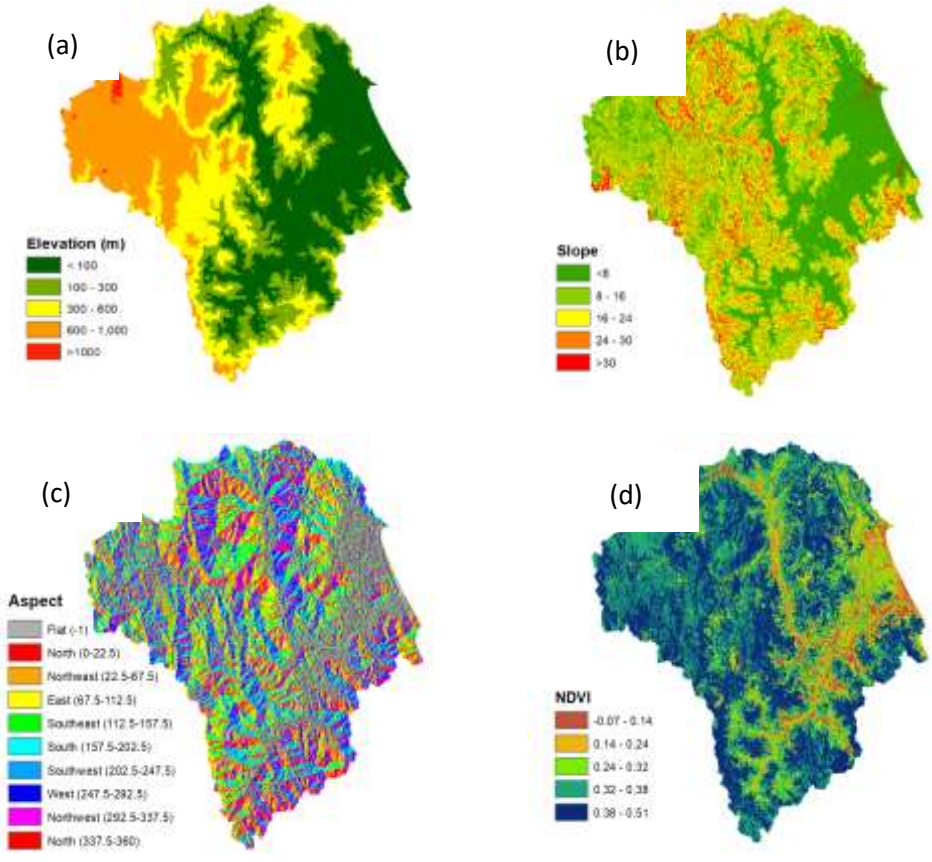

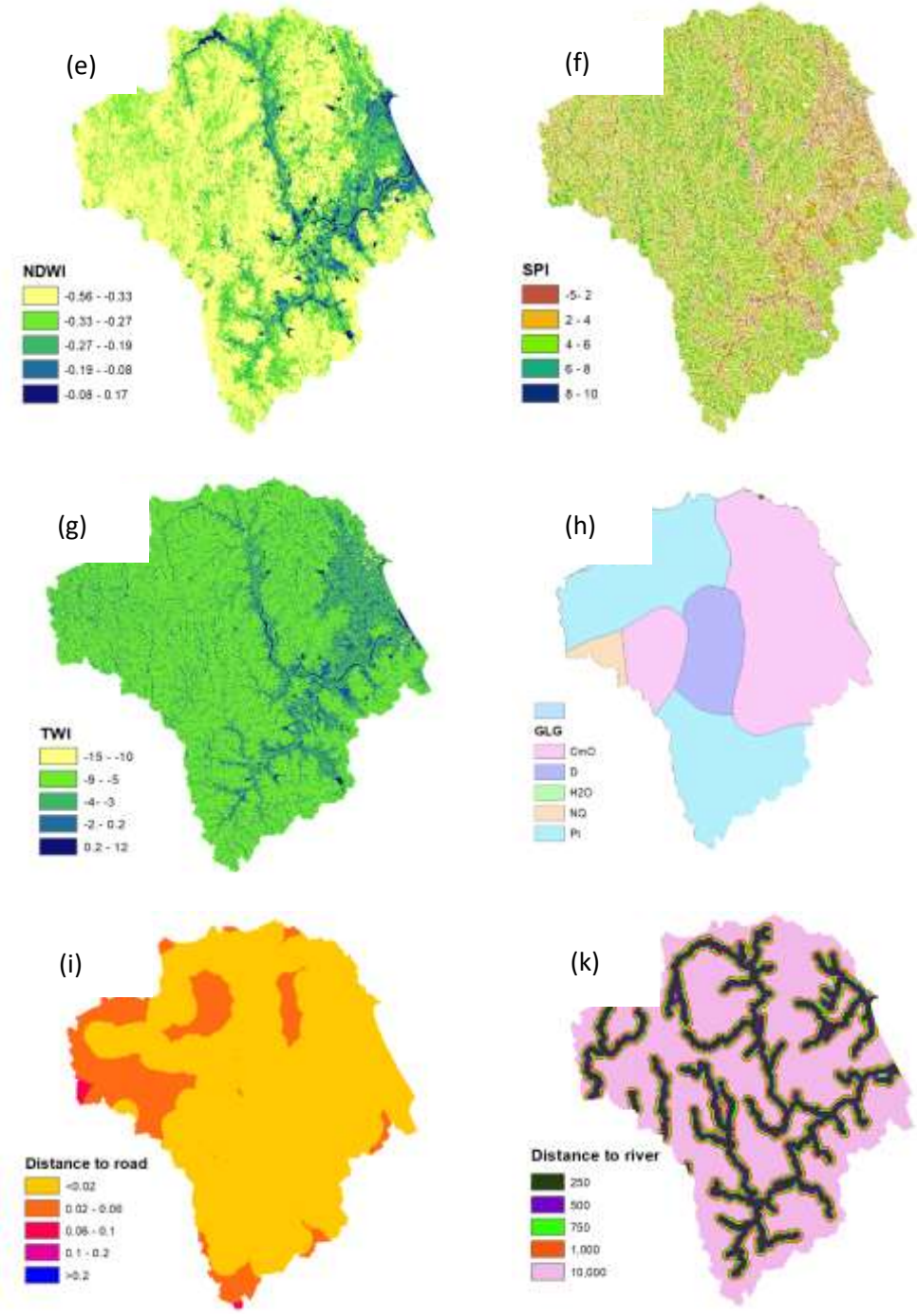

Figure 4: *The influencing factors related to landslides*

3.2. Landslides susceptibility maps and validation

Landslide susceptibility maps for the study area were developed using factor weights derived from the AHP and Fuzzy-AHP methods. Figure 5 presents the resulting susceptibility maps, while Table 7 summarizes the area coverage and percentage distribution across different susceptibility zones. The results from both

methods show minimal differences in the high and very high susceptibility zones. Notably, historical landslide events align closely with areas classified as very highly susceptible, underscoring the effectiveness of both AHP and Fuzzy-AHP techniques in assessing landslide risk in similar terrains.

The LSM generated using the AHP method (Figure 5a) categorizes the region into five susceptibility classes. According to Table 7, approximately 34.6% of the area falls within the very low susceptibility zone, 24.6% in the low zone, and 25.6% in the moderate zone. Areas classified as high and very high susceptibility account for 8.7% and 6.4%, respectively.

In comparison, the Fuzzy-AHP-based LSM (Figure 5b) indicates that 20.1% of the area is classified as very low susceptibility, 34.8% as low, and 30.1% as moderate. High and very high susceptibility zones cover 9% and 6.1% of the area, respectively.

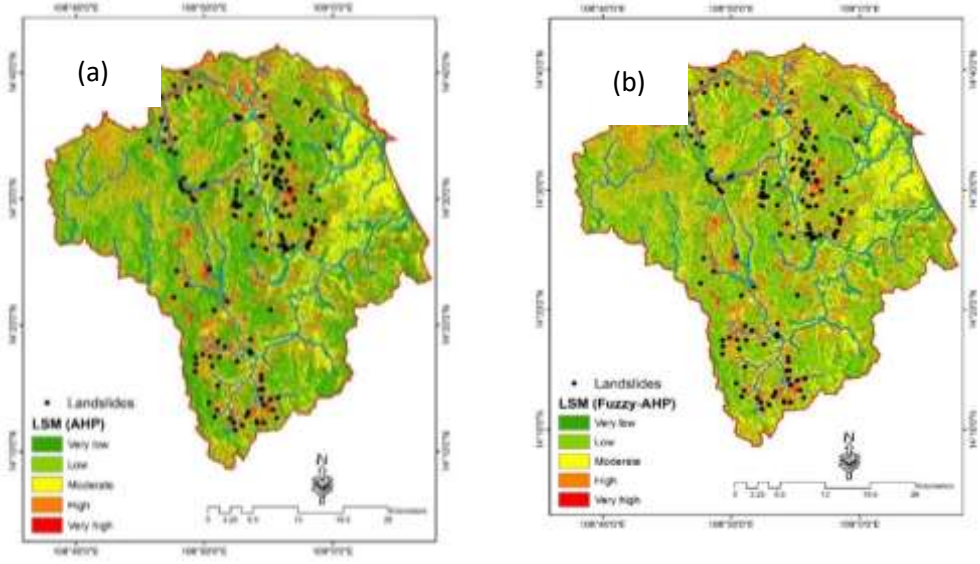

***Figure 5**: The landslide susceptibility maps using the AHP and Fuzzy-AHP*

***Table 7:** The area coverage and percentage of the landslide susceptibility areas.*

Class	Landslide susceptibity zone	AHP		Fuzzy-AHP	
		Area coverange (ha)	Area coverange (%)	Area coverange (ha)	Area coverange (%)
1	Very low	62913.24	34.6	36609.57	20.1
2	Low	44776.89	24.6	63159.93	34.8
3	Moderate	46468.8	25.6	54625.68	30.1

4	High	15892.56	8.7	16310.16	9.0
5	Very high	11665.71	6.4	11011.86	6.1

During the validation process, the AUC values obtained from the ROC curves were 0.827 (82.7%) for the AHP model and 0.871 (87.1%) for the Fuzzy-AHP model (Figure 6). These values indicate that the AHP method offers excellent predictive accuracy, while the Fuzzy-AHP method demonstrates superior performance. Overall, both approaches are effective and reliable for assessing landslide susceptibility in the study area.

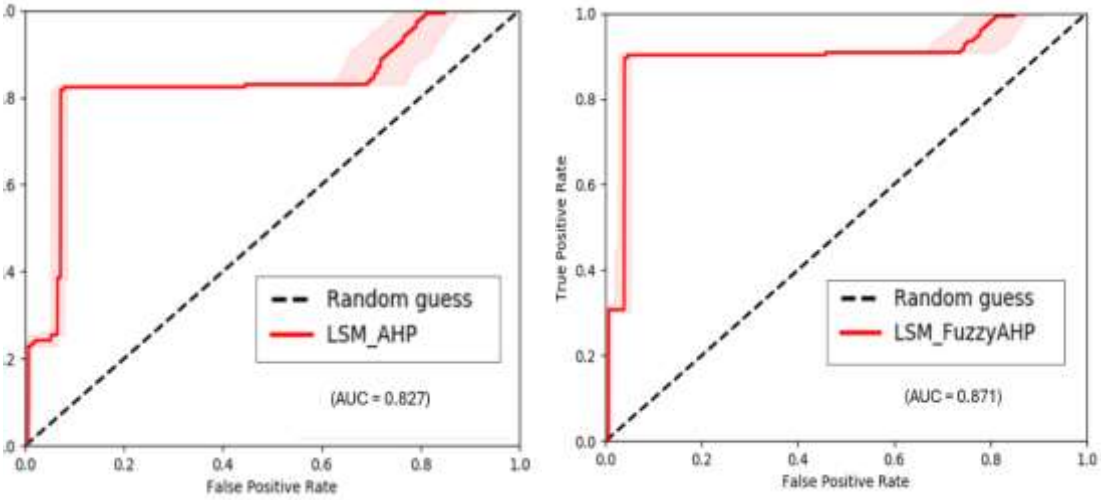

***Figure 6**: The ROC curve and AUC value*

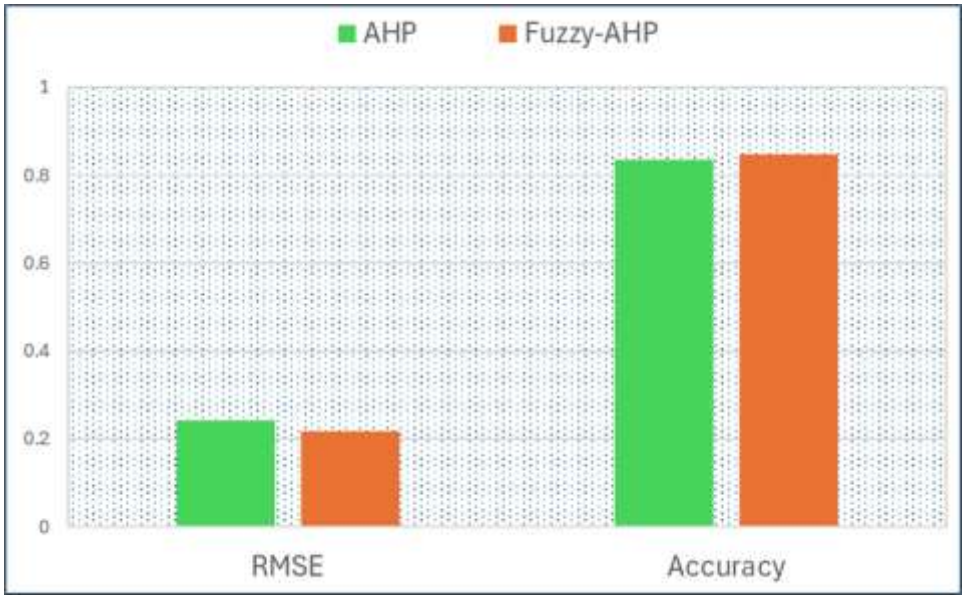

Figure 7: *The accuracy and RMSE values*

In addition to ROC-AUC analysis, other validation metrics such as accuracy and root mean square error (RMSE) were also used to assess model performance (Figure 7). The Fuzzy-AHP model demonstrated superior results, achieving an accuracy of 0.847 and an RMSE of 0.216. In comparison, the AHP model obtained an accuracy of 0.835 and an RMSE of 0.243. These findings indicate that while both models are effective for landslide susceptibility assessment, the Fuzzy-AHP model provides slightly better predictive performance.

4. Conclusions

Landslides are a recurrent natural hazard in Binh Dinh Province, Vietnam—particularly in the districts of Hoai An, Hoai Nhon, and An Lao, which have experienced numerous landslide events in recent years. This study applies the Analytical Hierarchy Process (AHP) and Fuzzy-AHP methods to develop landslide susceptibility maps for the region. Ten key conditioning factors were considered: elevation, slope, aspect, TWI, SPI, NDVI, NDWI, distance to roads, distance to rivers, and geological characteristics. The relative weight of each factor was determined using both AHP and Fuzzy-AHP approaches, resulting in two corresponding susceptibility maps.

The results indicate that approximately 15% of the study area falls within high and very high susceptibility zones, 30% in moderate zones, and the remainder in low or very low susceptibility zones. Validation through spatial analysis and ROC curves confirmed the strong performance of both models, with AUC values exceeding 0.80, overall accuracy above 0.8, and RMSE values around 0.2. These findings demonstrate that AHP and Fuzzy-AHP are reliable and effective tools for landslide susceptibility assessment in similar geographic and environmental contexts. The resulting susceptibility maps can serve as essential resources for government agencies and planners involved in landslide hazard management, supporting the development of mitigation strategies, early warning systems, and sustainable land-use planning practices.

Competing interests

The authors declare that they have no known competing financial interests or personal relationships that could have appeared to influence the work reported in this paper.

References

[1] M. J. Froude and D. N. Petley, “Global fatal landslide occurrence from 2004 to 2016,” *Natural Hazards and Earth System Sciences*, vol. 18, no. 8, pp. 2161–2181, Aug. 2018, doi: 10.5194/nhess-18-2161-2018.

[2] S. M. Fatemi Aghda, V. Bagheri, and M. Razifard, “Landslide Susceptibility Mapping Using Fuzzy Logic System and Its Influences on Mainlines in Lashgarak Region, Tehran, Iran,” *Geotechnical and Geological Engineering*, vol. 36, no. 2, pp. 915–937, 2018, doi: 10.1007/s10706-017-0365-y.

[3] A. V Thomas *et al.*, “Landslide Susceptibility Zonation of Idukki District Using GIS in the Aftermath of 2018 Kerala Floods and Landslides: a Comparison of AHP and Frequency Ratio

Methods," *Journal of Geovisualization and Spatial Analysis*, vol. 5, no. 2, p. 21, 2021, doi: 10.1007/s41651-021-00090-x.

[4] T. V Swetha and G. Gopinath, "Landslides susceptibility assessment by analytical network process: a case study for Kuttiyadi river basin (Western Ghats, southern India)," *SN Appl Sci*, vol. 2, no. 11, p. 1776, 2020, doi: 10.1007/s42452-020-03574-5.

[5] V. Vakhshoori and H. R. Pourghasemi, "A novel hybrid bivariate statistical method entitled FROC for landslide susceptibility assessment," *Environ Earth Sci*, vol. 77, no. 19, p. 686, 2018, doi: 10.1007/s12665-018-7852-1.

[6] D. Tien Bui, B. Pradhan, O. Lofman, and I. Revhaug, "Landslide susceptibility assessment in vietnam using support vector machines, decision tree, and nave bayes models," *Math Probl Eng*, vol. 2012, 2012, doi: 10.1155/2012/974638.

[7] S. A. Abu El-Magd, S. A. Ali, and Q. B. Pham, "Spatial modeling and susceptibility zonation of landslides using random forest, naïve bayes and K-nearest neighbor in a complicated terrain," *Earth Sci Inform*, vol. 14, no. 3, pp. 1227–1243, 2021, doi: 10.1007/s12145-021-00653-y.

[8] A. M. Youssef, H. R. Pourghasemi, Z. S. Pourtaghi, and M. M. Al-Katheeri, "Landslide susceptibility mapping using random forest, boosted regression tree, classification and regression tree, and general linear models and comparison of their performance at Wadi Tayyah Basin, Asir Region, Saudi Arabia," *Landslides*, vol. 13, no. 5, pp. 839–856, 2016, doi: 10.1007/s10346-015-0614-1.

[9] S. Paryani, A. Neshat, and B. Pradhan, "Spatial landslide susceptibility mapping using integrating an adaptive neuro-fuzzy inference system (ANFIS) with two multi-criteria decision-making approaches," *Theor Appl Climatol*, vol. 146, no. 1, pp. 489–509, 2021, doi: 10.1007/s00704-021-03695-w.

[10] Y. Wang, Z. Fang, and H. Hong, "Comparison of convolutional neural networks for landslide susceptibility mapping in Yanshan County, China," *Science of The Total Environment*, vol. 666, pp. 975–993, 2019, doi: https://doi.org/10.1016/j.scitotenv.2019.02.263.

[11] S. B. Bhagya *et al.*, "Landslide Susceptibility Assessment of a Part of the Western Ghats (India) Employing the AHP and F-AHP Models and Comparison with Existing Susceptibility Maps," *Land (Basel)*, vol. 12, no. 2, Feb. 2023, doi: 10.3390/land12020468.

[12] S. B. Bhagya *et al.*, "Landslide Susceptibility Assessment of a Part of the Western Ghats (India) Employing the AHP and F-AHP Models and Comparison with Existing Susceptibility Maps," *Land (Basel)*, vol. 12, no. 2, Feb. 2023, doi: 10.3390/land12020468.

[13] C. Kincal and H. Kayhan, "A Combined Method for Preparation of Landslide Susceptibility Map in Izmir (Türkiye)," *Applied Sciences (Switzerland)*, vol. 12, no. 18, Sep. 2022, doi: 10.3390/app12189029.

[14] C. Marzban, "The ROC Curve and the Area under It as Performance Measures."

[15] A. Wubalem, "Landslide susceptibility mapping using statistical methods in Uatzau catchment area, northwestern Ethiopia," *Geoenvironmental Disasters*, vol. 8, no. 1, p. 1, 2021, doi: 10.1186/s40677-020-00170-y.

[16] D. Christie and S. Neill, "Measuring and Observing the Ocean Renewable Energy Resource," in *Reference Module in Earth Systems and Environmental Sciences*, 2021. doi: 10.1016/B978-0-12-819727-1.00083-2.

[17] L. P, M. C, A. Mathew, and P. R. Shekar, "Machine learning and deep learning-based landslide susceptibility mapping using geospatial techniques in Wayanad, Kerala state, India," *HydroResearch*, vol. 8, pp. 113–126, Jan. 2025, doi: 10.1016/j.hydres.2024.10.001.

[18] C. Kincal and H. Kayhan, "A Combined Method for Preparation of Landslide Susceptibility Map in Izmir (Türkiye)," *Applied Sciences (Switzerland)*, vol. 12, no. 18, Sep. 2022, doi: 10.3390/app12189029.

[19] A. Hammad Khaliq *et al.*, "Spatiotemporal landslide susceptibility mapping using machine learning models: A case study from district Hattian Bala, NW Himalaya, Pakistan," *Ain Shams Engineering Journal*, vol. 14, no. 3, Apr. 2023, doi: 10.1016/j.asej.2022.101907.